ADVANCED MATERIALS INTERFACES

Supporting Information

for *Adv. Mater. Interfaces,* DOI: 10.1002/admi.202000672

Rational Design of Transparent Nanowire Architectures with Tunable Geometries for Preventing Marine Fouling

Jing Wang, Sudarat Lee, Ashley R. Bielinski, Kevin A. Meyer, Abhishek Dhyani, Alondra M. Ortiz-Ortiz, Anish Tuteja, and Neil P. Dasgupta**

Supporting Information

Rational Design of Transparent Nanowire Architectures for Preventing Marine Fouling

Jing Wang, Sudarat Lee, Ashley R. Bielinski, Kevin A. Meyer, Abhishek Dhyani, Alondra M. Ortiz-Ortiz, Anish Tuteja, Neil P. Dasgupta**

Dr. Jing Wang, Dr. Sudarat Lee, Dr. Ashley R. Bielinski, Alondra M. Ortiz-Ortiz, Prof. Neil P. Dasgupta,
Department of Mechanical Engineering, University of Michigan, Ann Arbor, Michigan 48109, United States
Email: ndasgupt@umich.edu
Dr. Kevin A. Meyer,
School for Environment and Sustainability, University of Michigan, Ann Arbor, Michigan 48109, United States
Abhishek Dhyani, Prof. Anish Tuteja,
Department of Macromolecular Science and Engineering, University of Michigan, Ann Arbor, Michigan 48109, United States
Biointerfaces Institute, University of Michigan, Ann Arbor, Michigan 48109, United States
Prof. Anish Tuteja,
Department of Materials Science and Engineering, University of Michigan, Ann Arbor, Michigan 48109, United States
Department of Chemical Engineering, University of Michigan, Ann Arbor, Michigan 48109, United States
Email: atuteja@umich.edu

Shear flow setup: To test the durability of the NWs under shear flow, we built an open channel flow setup (**Fig. S3**), which generates shear forces on the surface to study fouling release [1]. The applied shear flow could also in part simulate the shear forces experienced by surfaces when they are submerged in the ocean. Specifically, the shear flow setup can generate water flow with a flow rate up to 2 gpm. The flow rate is controlled by a throttle valve. The open channel was made of acrylic with 1-m in length (L_c) and 27-mm in width (w).

At the highest flow rate (2 gpm), we can calculate the required length for fully developed flow by calculating the Reynolds number (Re = $4VR/v$) and Froude number (Fr = $V/(gh)^{1/2}$), where R is hydraulic diameter, V is the flow velocity, v is the kinetic viscosity, g is the gravity constant, and h is the flow height. The hydraulic diameter is R = A/P, where A is the flow cross-sectional area, and $P = w+2h$ is the wetted perimeter. For open channel flow, the length of the flow development zone (L) can be determined using the analysis described by Kirkgöz and Ardiçlioğlu (1997) [2]:

$$L/h = 76 - 0.001\mathrm{Re/Fr} \qquad \text{(S1)}$$

The wall shear on the bed of the channel can be described by the equation from Guo and Julien (2005) [3]:

$$\frac{\tau_b}{\rho g h S} = \frac{4}{\pi}\tan^{-1}\exp\left(-\frac{\pi h}{w}\right)+\frac{\pi}{4}\frac{h}{w}\exp\left(-\frac{h}{w}\right) \qquad \text{(S2)}$$

where τ_b is the wall shear in the channel bed, ρ is the density, S is the slope of the channel (1:5000). The wall shear (τ_b), the development zone (L) and all dimensionless numbers (We and Fr) are calculated as shown in **Table S1**. The NW geometry did not change after 1-hour exposure to the shear flow with the maximum flow rate (**Fig. S4**).

Fluid and acoustic cleaning on algae fouled NWs: We performed experiments to evaluate the impact, and acoustic stability of NWs by cleaning the attached biofilm with a strong water jet from a squeeze bottle and exposing the sample to ultrasonication. As confirmed by scanning

electron microscope (SEM) (**Fig. S5**) analysis, the NWs were not damaged through the processes of the attachment and subsequent detachment of biofilm, water jet cleaning (20 min), and sonication (20 min).

Haze measurements on NW samples: Haze measurements can be used describe the fraction of light scattered when incident light passes through a transparent sample [4]. Experimentally, this was accomplished by measuring the total transmittance of the NW sample (T_s) and the diffusion rate of both the NW sample (DT_s) as well as the instrument (DT_{ins}) using a UV-vis spectrophotometer equipped with an integrating sphere. The haze percentage was calculated using the following equation:

$$\text{Haze} = (DT_s - DT_{ins})/T_s \times 100\% \qquad \text{(S3)}$$

Haze measurements of various geometries tested in this study are shown in **Figure S7**.

Environmental factors on fouling performance: In the ocean environment, the nature of marine biofouling will vary significantly with factors including geographic location, season, lighting, etc. While a comprehensive study of the impact of all these variables is beyond the scope of this study, one consequence of these environmental variables is a variation in the initial concentration of the marine species in the vicinity of the fouled surfaces. Therefore, the effect of initial algae concentration on the fouling behavior on various NW surfaces was further studied.

To vary the initial concentration, the mass of the wet biomass introduced to the fouling test was reduced by 50%. A greater reduction in fouling area fraction (~60%) was observed on NWs in the Wenzel state under these low-concentration conditions compared to a high-concentration environment (~50%) (see **Fig. S11** and **Fig. 4b**). Furthermore, the duration of superhydrophobicity was longer for the low-concentration environment (8~14 days) than the high concentration (6~12 days; see **Fig. S18**). In addition, the superhydrophobic duration increases linearly with the volume of the air layer on the NWs regardless of the initial

concentration. Overall, the trends described in the manuscript were fully consistent in the low-concentration environment, which illustrates that the mechanistic understanding of the coupled geometric, wetting, and fouling behavior of the NW architectures is maintained.

Underwater superhydrophobic duration: The duration of underwater superhydrophobicity can be modeled by Fick's law of diffusion. The total time (τ) the air layer takes to diffuse from the NW textures into water depends on the total volume of the air layer (V) and the diffusion volume flux (k). It is known that $k \propto D^{n_1}$ [5] and $D \propto p^{n_2}$ [6], where D is the diffusivity, p is the hydrostatic pressure, and n_1 and n_2 are experimental values, Therefore, the duration of underwater superhydrophobicity can be expressed as:

$$\tau = \frac{V}{dV/dt} = \frac{V}{kA} \sim \frac{V}{D^{n_0}} \sim Vp^n \qquad \text{(S4)}$$

where n is an experimental constant depending on water properties (e.g., surface tension, oxygen and nitrogen level, etc.) and any present contaminants (e.g., biological species, ionic concentration, organic contaminants, etc.).

Supporting Video:

Supporting Video S1 shows the water repellency of the superhydrophobic NW-coated glass dome. The blue liquid drop is dyed DI water.

Supporting Figures:

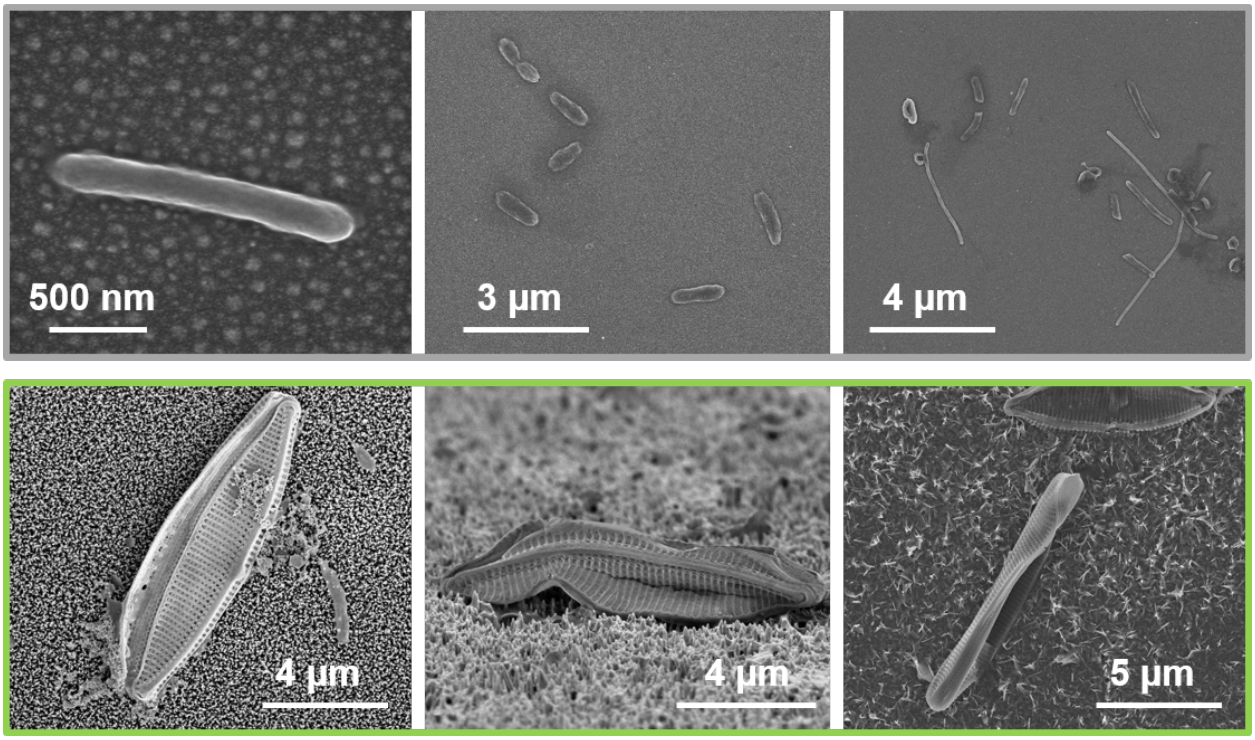

Figure S1. Scanning electron microscope (SEM) images of cyanobacteria (gray box) and diatoms (green box) on the NWs. A variety of cyanobacteria and diatoms were observed from these SEM images, indicating the multi-species marine fouling environment used in this study.

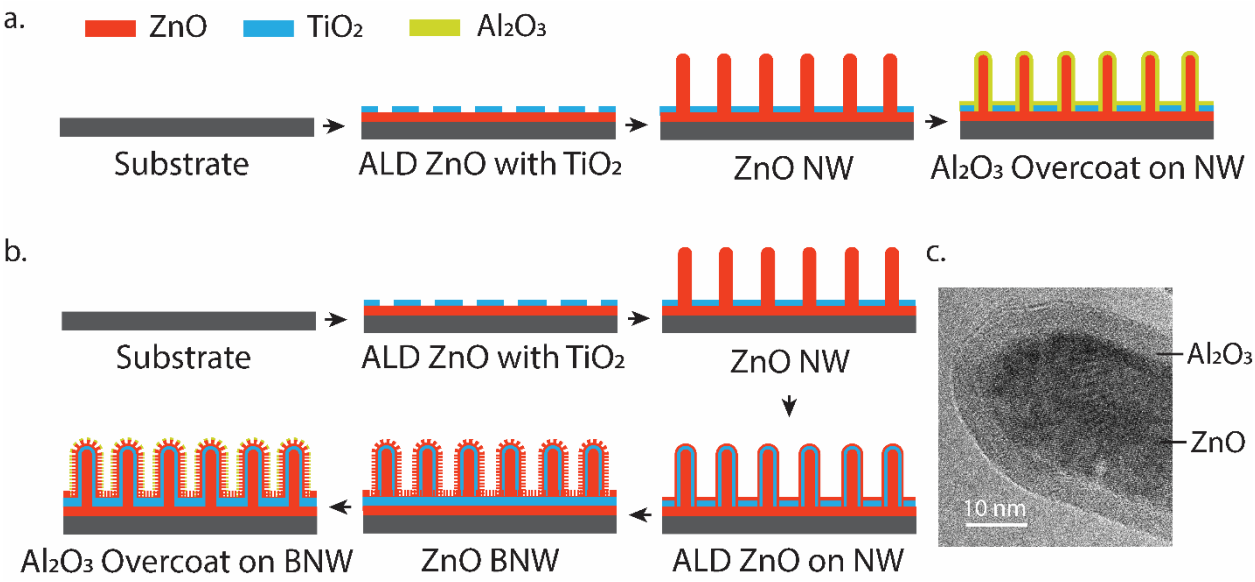

Figure S2. Fabrication processes of core-shell NWs and BNWs. a, Fabrication processes of NWs with controlled length and spacing. b, Fabrication processed of BNWs. c. Transmission electron microscopy (TEM) image of a core-shell NW.

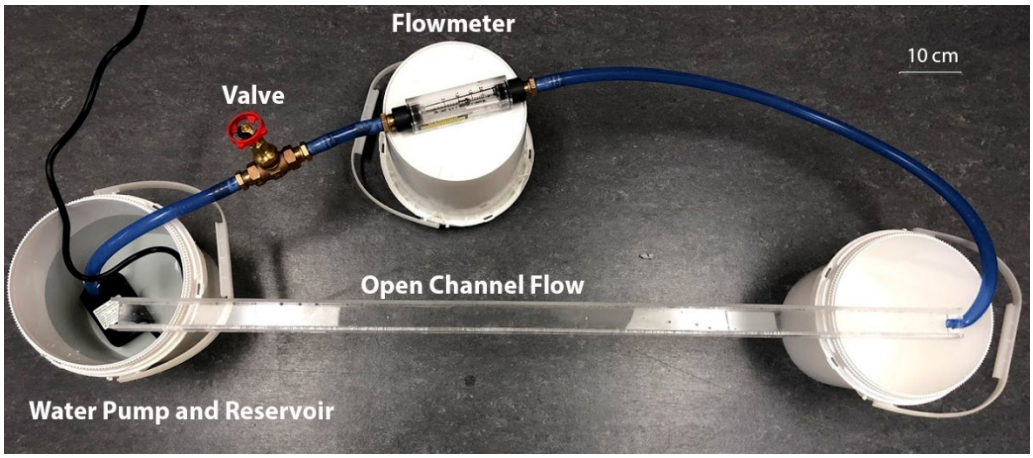

Figure S3. Shear flow setup. Open channel flow composed of water reservoir, pump, valve, flowmeter, and the flow channel. The flow rate is 0 to 2 gpm.

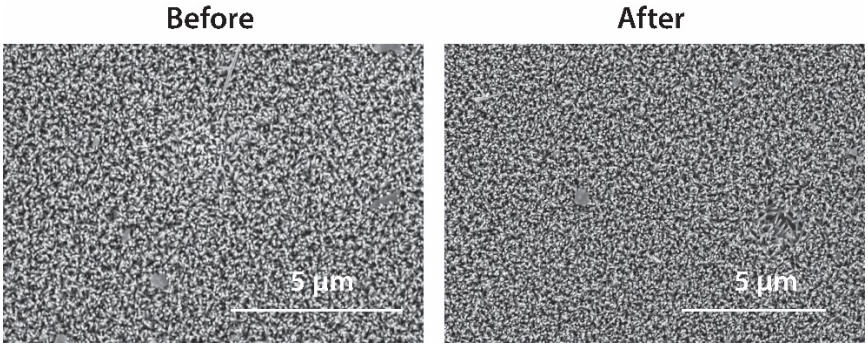

Figure S4. Scanning electron microscope (SEM) images of NWs before and after shear flow with a flow rate of 2 gpm.

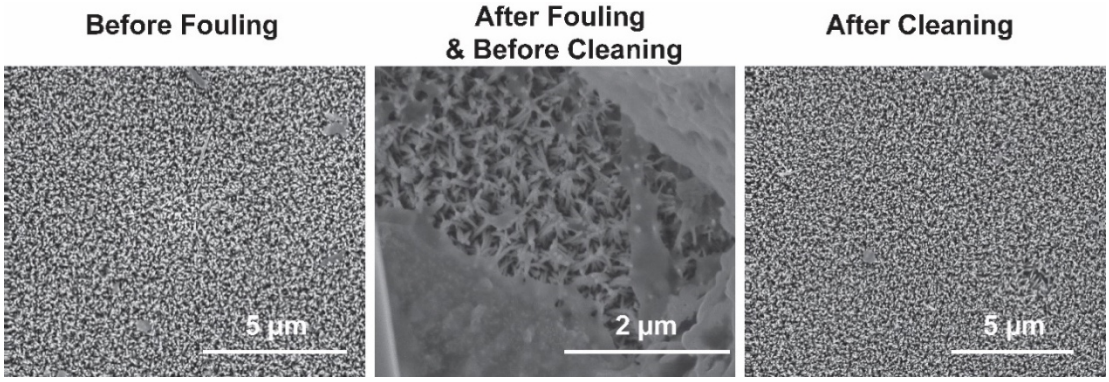

Figure S5. SEM images of NWs before fouling, after fouling and before cleaning, and after cleaning.

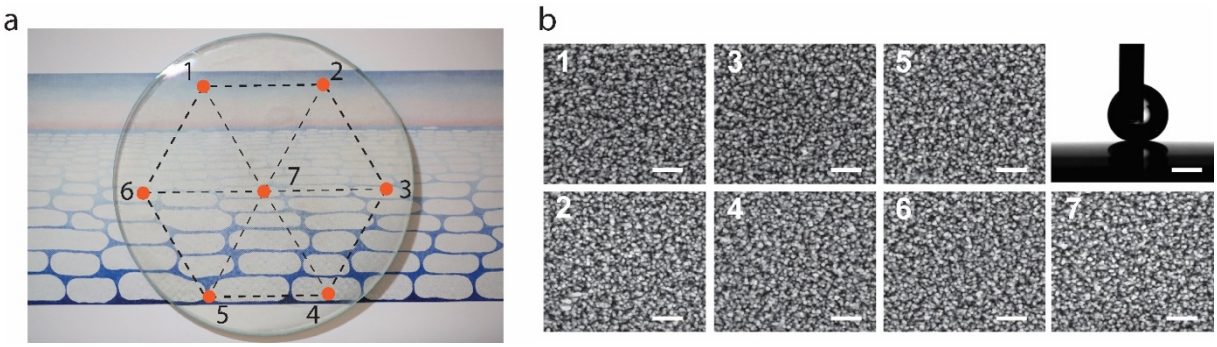

Figure S6. Fabrication and characterization of NW growth on curved surfaces. a, Optical photograph demonstrating the transparency of the NW-coated watch glass (diameter: 70 mm). The background is a postcard with the painting of Sky Above Clouds IV, 1965 from Georgia O'Keeffe. b, SEM images showed NW growth on 7 different points on the watch glass. The optical image of a water droplet (~5 μL) sitting on the top center of the superhydrophobic watch glass. The scale bars for all SEM images are 500 nm, and the scale bar to the optical image of the droplet is 5 mm.

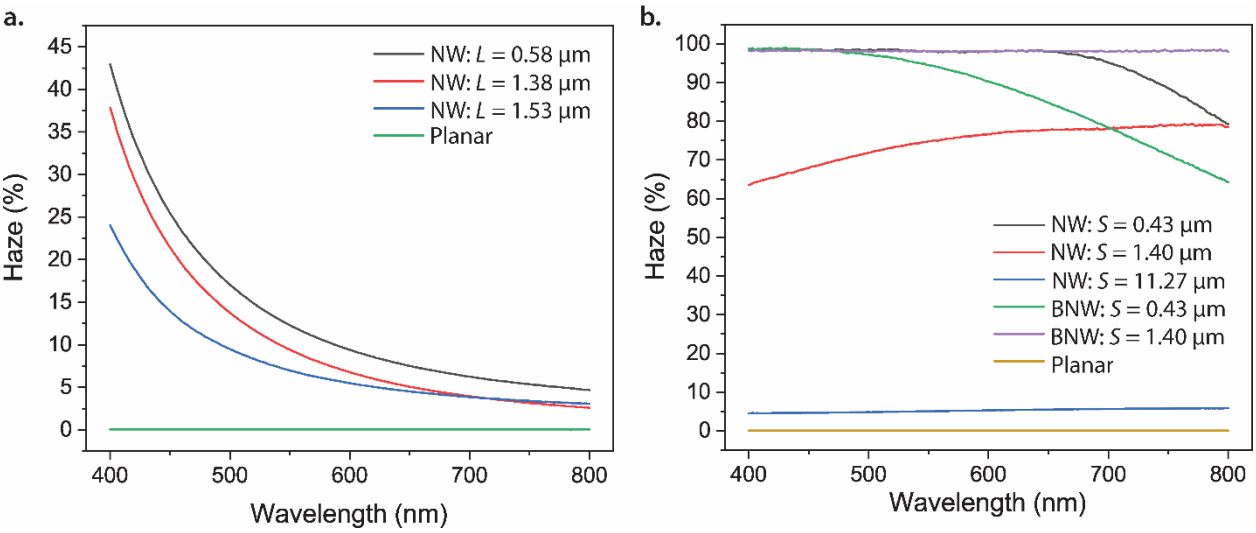

Figure S7. Haze measurement on different surfaces. a, Haze measurements on NWs with different lengths (i.e., growth time) compared with the planar control. b, Haze measurements on NWs with different spacings and branching geometries compared with the planar control.

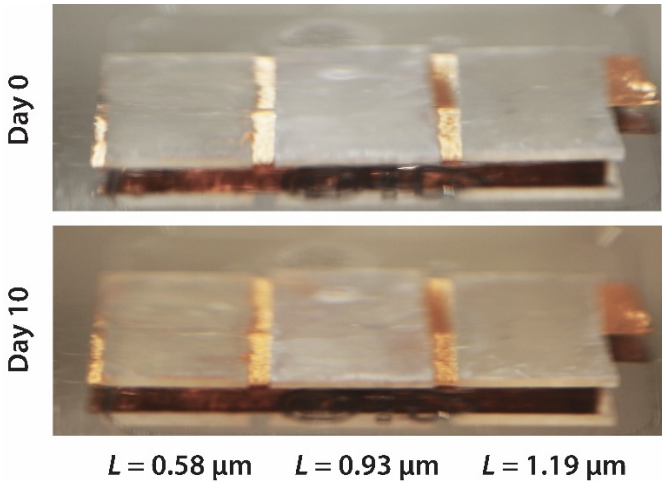

Figure S8. Optical images of superhydrophobic NWs underwater with a depth of 300 mm for 10 days.

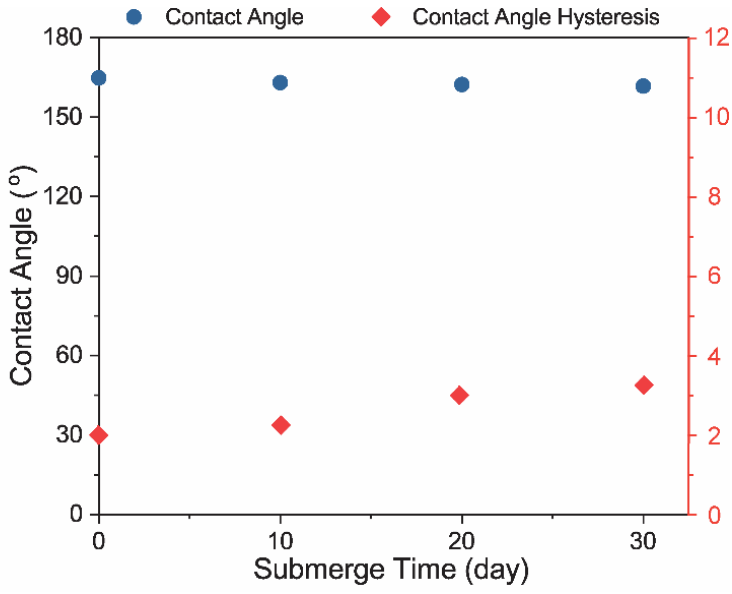

Figure S9. Contact angle and contact angle hysteresis measurement on NWs submerged in synthetic seawater for 30 days.

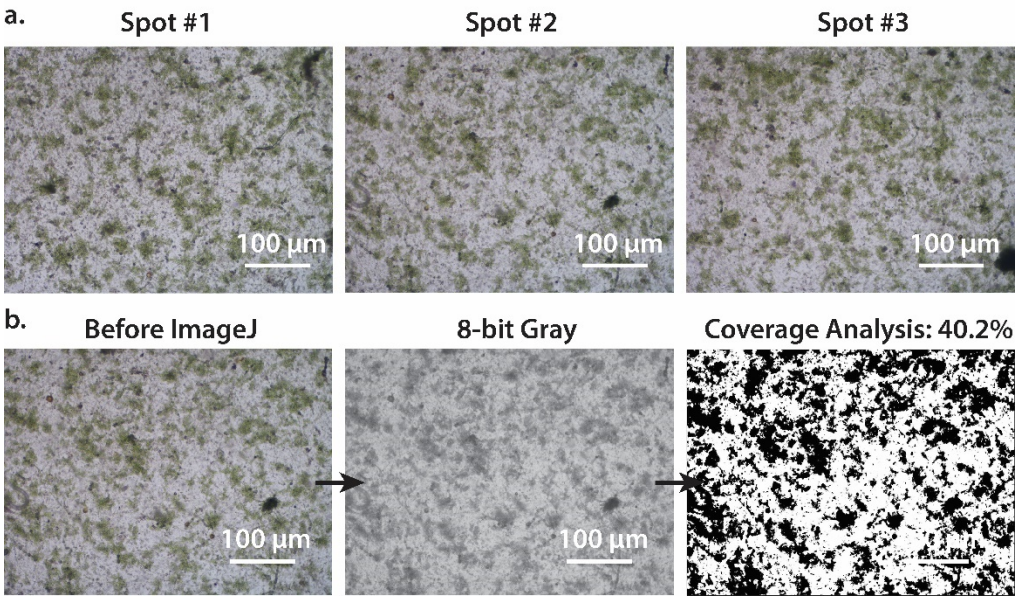

Figure S10. Microscopic image analysis for marine algal fouling test. a, Microscopic images at three different measurement spots on the sample after 20 days of fouling. b, ImageJ analysis process on the microscopic image to obtain the coverage fraction information of the biofouling.

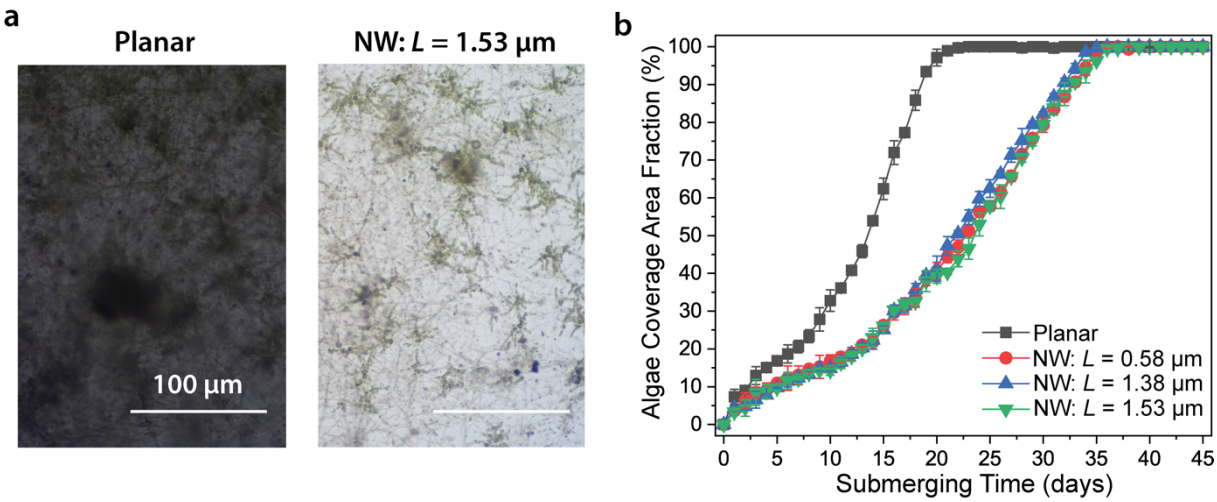

Figure S11. Marine algal fouling performance on hydrophilic NWs with different lengths in low concentration algae environment. a, Optical microscopy images on NW surfaces in the Wenzel state after 20 days of the algae fouling. b, Algae coverage area fraction on NWs with different lengths in the Wenzel state for 45 days.

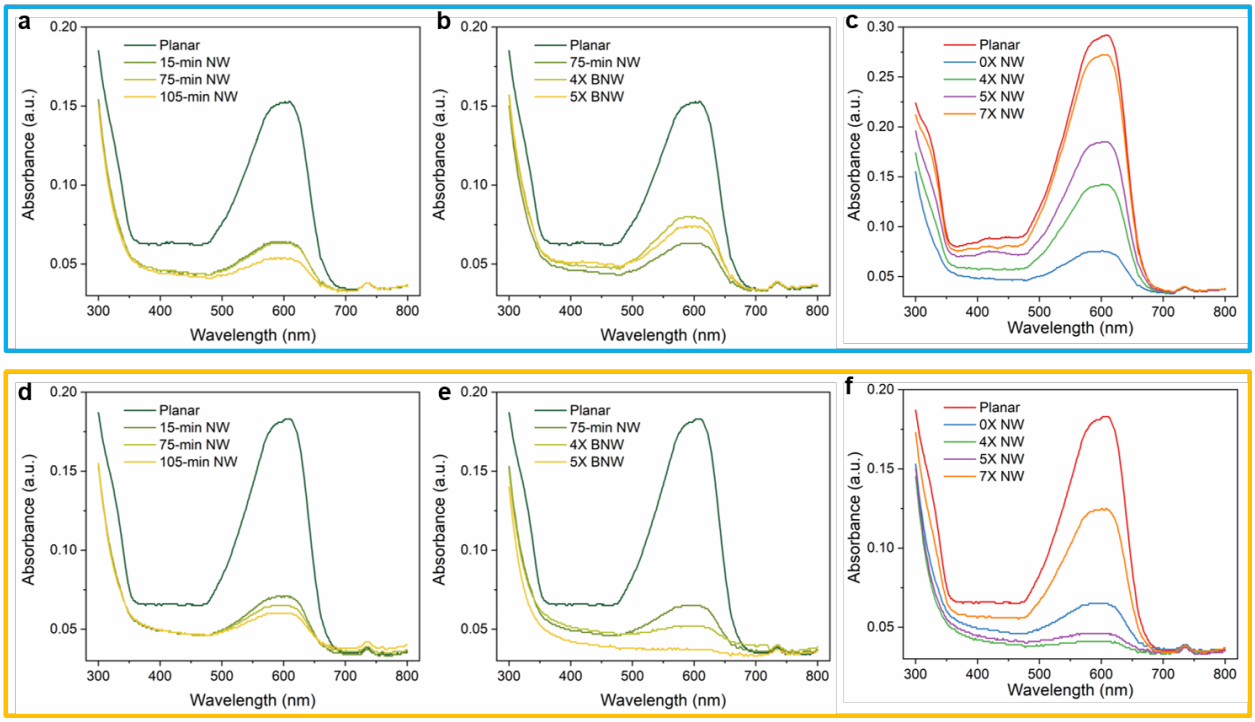

Figure S12. Optical density of NWs with different geometries and chemistry after 20 days fouling test. a, b, and c, Optical density measurements (i.e., absorbance) on hydrophilic NWs and planar control surfaces after 20 days of an algae fouling test. d, e, and f, Optical density measurements (i.e., absorbance) on hydrophobic NWs and planar control after 20 days of an algae fouling test.

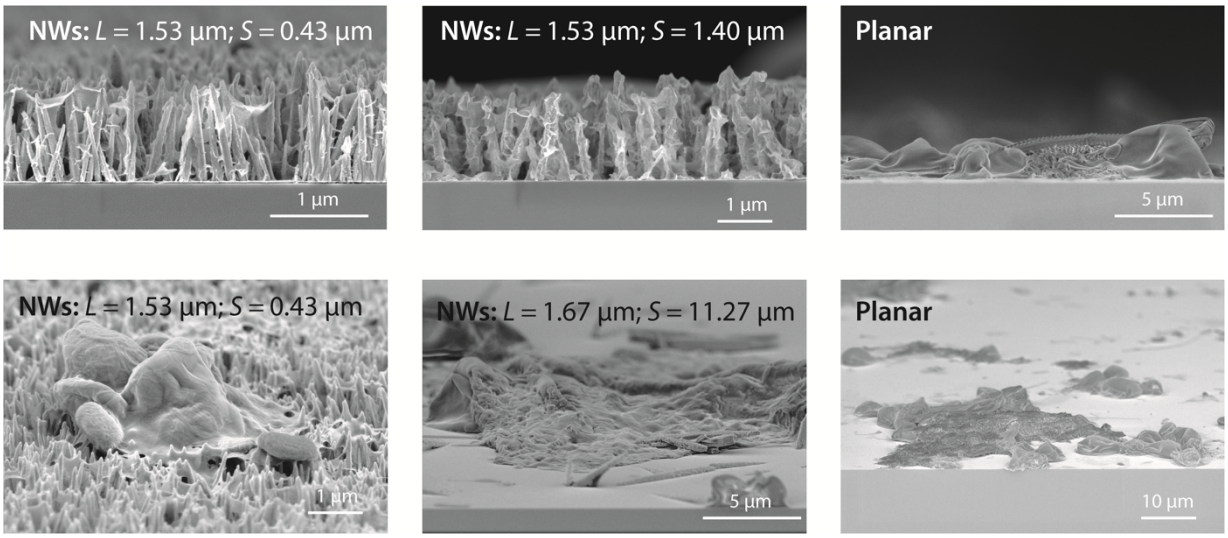

Figure S13. SEM images of algal fouling on hydrophilic NWs with different inter-NW spacings, including planar surfaces.

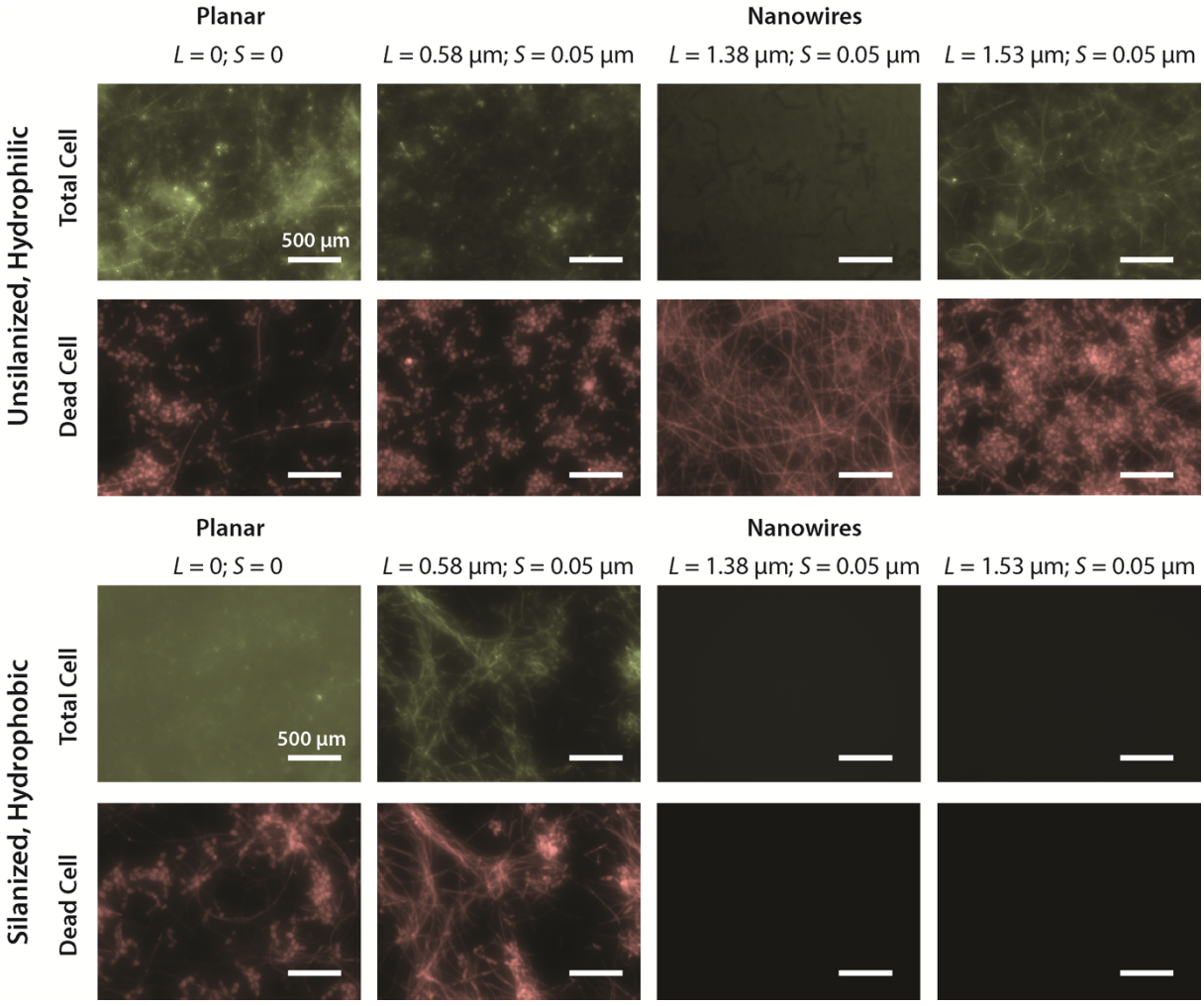

Figure S14. Fluorescent microscopy images on hydrophilic and hydrophobic NWs with different lengths and planar control surfaces with the same surface chemistry correspondingly after 10 days of algae fouling testing.

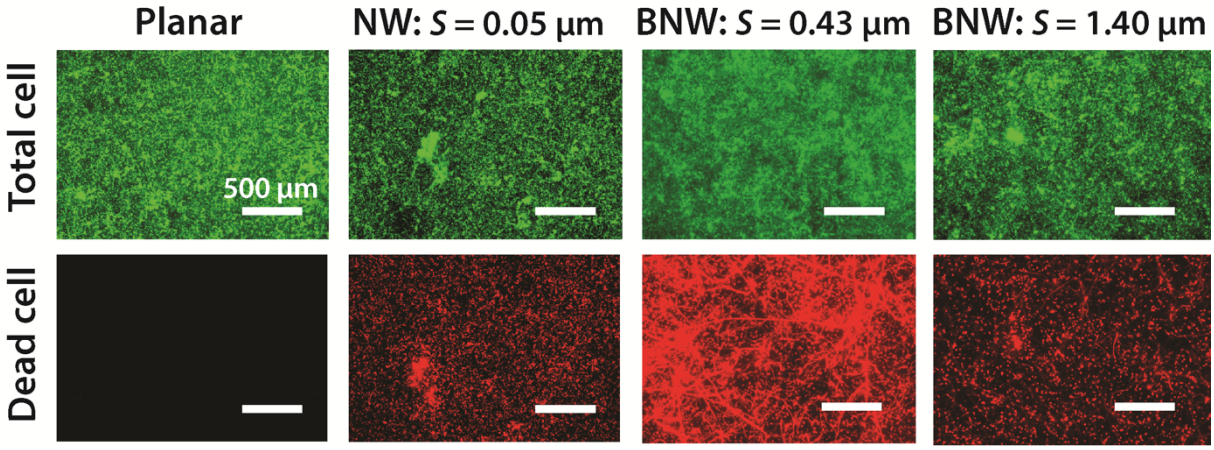

Figure S15. Fluorescent microscope images on hydrophilic NWs with tunable branching geometries after 5 days of algae fouling testing.

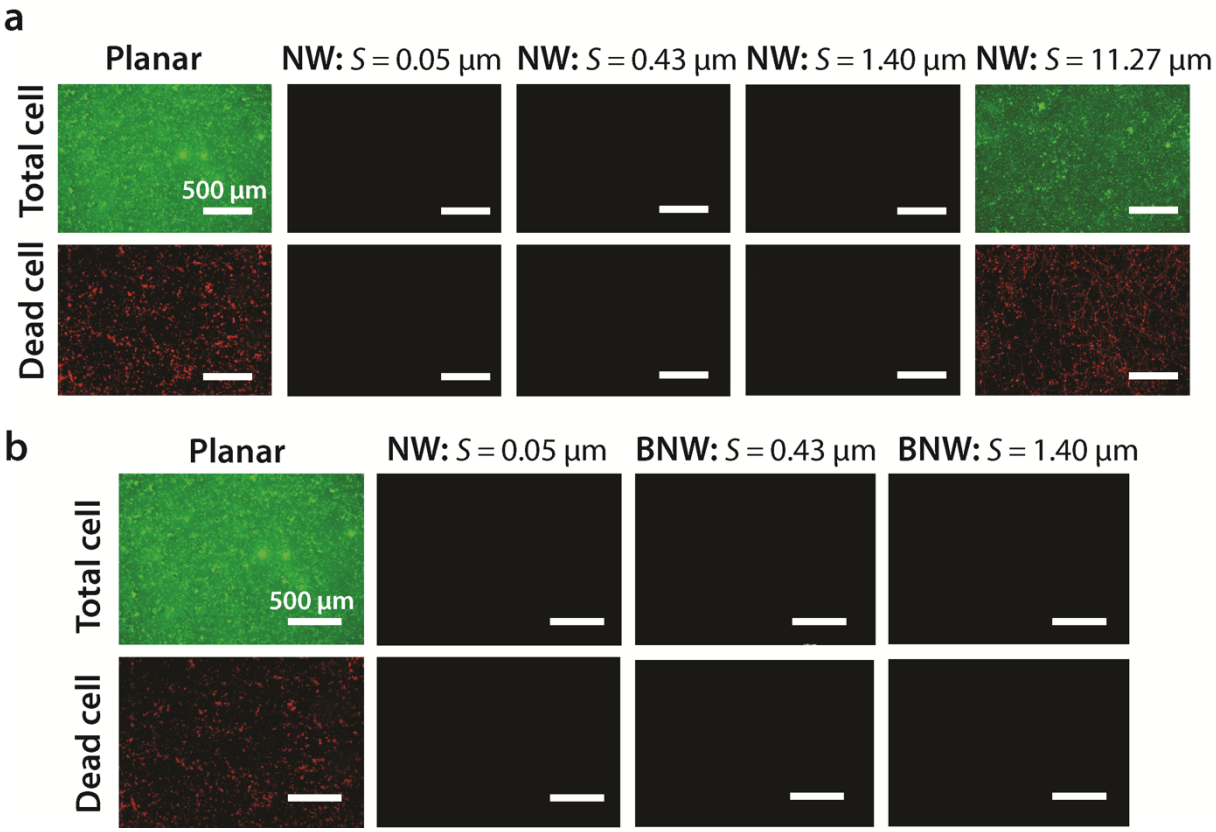

Figure S16. Fluorescent microscopic images of hydrophobic NWs with (a) different spacings and (b) hierarchies after 5 days of algae fouling testing.

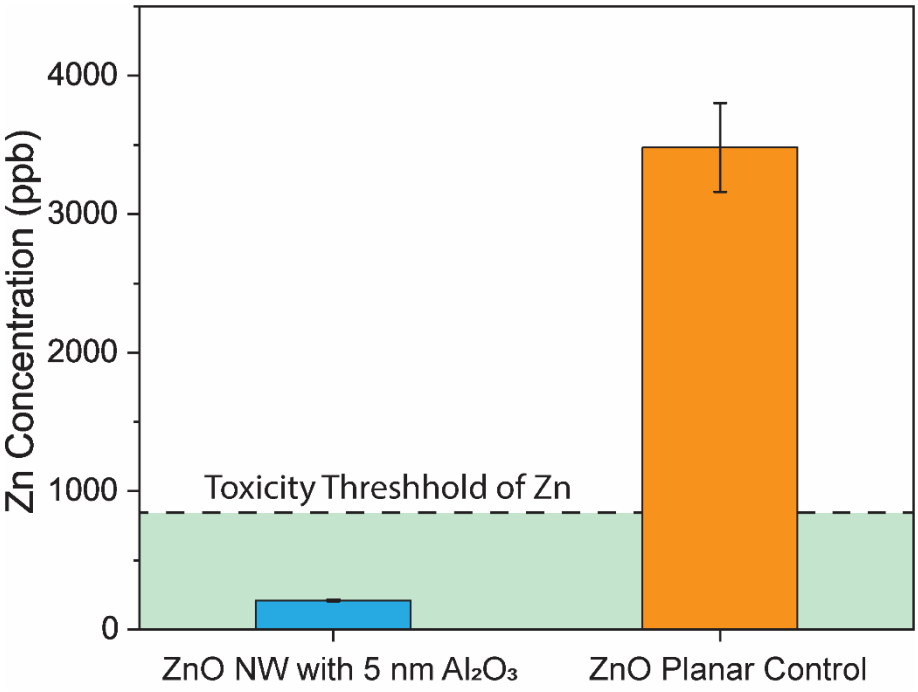

Figure S17. Zn ion concentration measurement by ICP-MS. The 5-nm Al_2O_3 overcoat prevented the ZnO NWs from dissolving into the solution, while a planar ZnO control sample without the Al_2O_3 overcoat dissolves at a much higher rate.

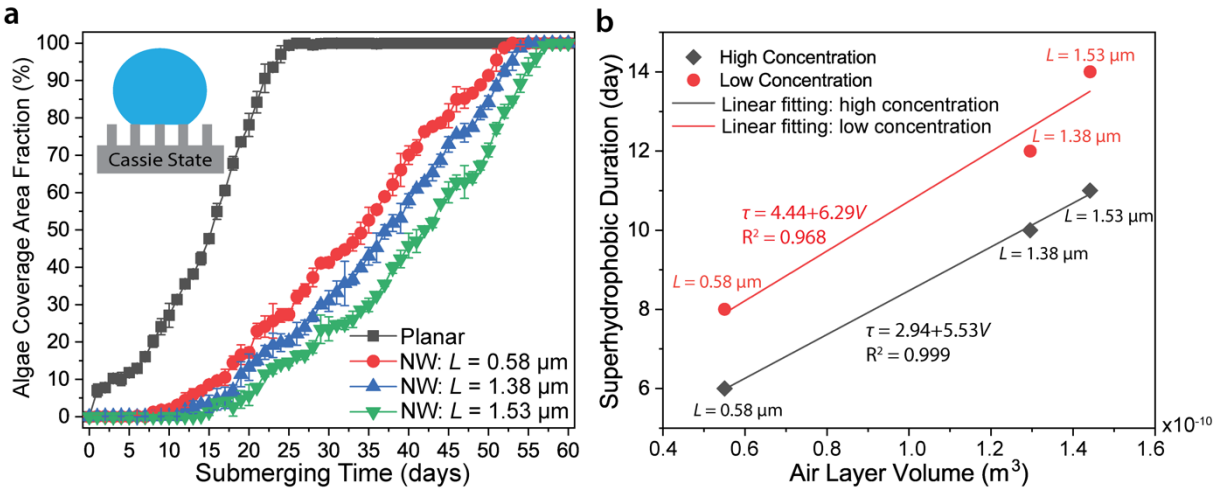

Figure S18. Algal fouling on NWs with different lengths under different environmental conditions. a, Algae coverage area fraction on NWs with different lengths in the Cassie state for 60 days. Errors bars were obtained from at least 3 independent measurements. b, Linear fitting of superhydrophobicity duration vs air layer volume with different NW lengths and under different conditions.

Supporting Table:

Table S1. Example of flow parameters in highest flow rate (2 gpm).

Flow rate (m^3/s)	**Flow height h (m)**	**Re**	**Fr**	**Developed zone L (m)**	**Wall Shear τ_b (Pa)**
1.26×10^{-4}	4.3×10^{-3}	1067	4.94	0.34	0.35

Table S2. Contact angle, contact angle hysteresis, and calculated sliding angle of NWs with the same inter-NW spacing (S = 0.05 μm) and different NW length (L).

NW Samples	**Advancing Angle (º)**	**Receding Angle (º)**	**Contact Angle hysteresis (º)**	**Calculated sliding angle (º)**
***L* = 0.58 μm**	165.2±0.1	163.3±0.2	1.9±0.2	0.5±0.1
***L* = 0.93 μm**	166.1±0.1	164.8±0.1	1.3±0.1	0.4±0.1
***L* = 1.12 μm**	166.2±0.1	164.9±0.1	1.3±0.1	0.4±0.1
***L* = 1.19 μm**	167.2±0.1	165.9±0.2	1.3±0.2	0.2±0.1
***L* = 1.38 μm**	167.0±0.1	165.9±0.2	1.1±0.2	0.2±0.1
***L* = 1.53 μm**	167.0±0.1	165.9±0.2	1.1±0.2	0.2±0.1

Table S3. Contact angle, contact angle hysteresis, and calculated sliding angle of NWs with the same NW length (L = 1.20 μm) and different inter-NW spacing (S).

NW Samples	**Advancing Angle (º)**	**Receding Angle (º)**	**Contact Angle hysteresis (º)**	**Calculated sliding angle (º)**
***S* = 0.05 μm**	167.2±0.1	165.9±0.2	1.3±0.2	0.2±0.1
***S* = 0.20 μm**	162.3±0.8	148.6±0.8	13.7±0.8	6.4±0.3
***S* = 0.43 μm**	163.3±0.7	153.5±1.2	9.8±1.0	4.4±0.4
***S* = 1.40 μm**	169.8±0.2	162.7±0.4	7.1±0.4	1.0±0.1
***S* = 4.39 μm**	136.3±0.3	0	136.3±0.3	pinned
***S* = 11.27 μm**	120.7±0.3	89.9±1.2	30.8±1.2	pinned

Table S4. Contact angle measurement on branched NWs.

Materials	**Advancing Angle (º)**	**Receding Angle (º)**	**Contact Angle (º)**	**Contact Angle hysteresis (º)**	**Calculated sliding angle (º)**
Hydrophilic BNWs (*S* = 0.43 μm)	0	0	0	pinned	pinned
Hydrophilic BNWs (*S* = 1.40 μm)	0	0	0	pinned	pinned
Hydrophobic BNWs (*S* =	162.6±1.0	160.0±0.5	161.7±0.4	2.6±1.0	0.7±0.1

0.43 µm)					
Hydrophobic BNWs (*S* = 1.40 µm)	164.1±0.6	161.3±0.4	163.2±0.3	2.8±0.6	0.8±0.1

Table S5. Contact angle and contact angle hysteresis of NWs with NW length (*L* = 1.20 µm) and inter-NW spacing (*S* = 0.05 µm) before and after 1-year of ambient air exposure.

NW Samples	Advancing Angle (º)	Receding Angle (º)	Contact Angle hysteresis (º)	Static Contact Angle (º)
Before	162.6±0.1	160.0±0.3	2.6±0.3	161.9±0.1
After	162.1±0.2	160.3±0.4	1.8±0.4	161.5±0.2

Reference

[1] J. A. Finlay, M. P. Schultz, G. Cone, M. E. Callow, J. A. Callow, *Biofouling* **2013**, 29, 401.
[2] M. S. Kirkgöz, M. Ardiçlioğlu, *Journal of Hydraulic Engineering* **1997**, 123, 1099.
[3] J. Guo, P. Y. Julien, *Journal of hydraulic engineering* **2005**, 131, 30.
[4] D. K. Yang, L. C. Chien, J. Doane, *Applied physics letters* **1992**, 60, 3102.
[5] K. Holmén, P. Liss, *Tellus B: Chemical and Physical Meteorology* **1984**, 36, 92.
[6] D. Himmelblau, *Chemical Reviews* **1964**, 64, 527.